JTTEE5 19:1238–1243
DOI: 10.1007/s11666-010-9544-6
1059-9630/$19.00 © ASM International

Effect of Nano-Sized TiN Additions on the Electrical Properties of Vacuum Cold Sprayed SiC Coatings

Y. Liu, Y.-Y. Wang, G.-J. Yang, J.-J. Feng, and K. Kusumoto

(Submitted March 9, 2010; in revised form July 25, 2010)

Three different contents of nano-sized TiN powers of 20 nm in size were added to nano-sized SiC powders of 40 nm. Vacuum cold spray (VCS) process was used to deposit SiC-TiN composite coatings on Al_2O_3 substrates. Microstructure and phase structure analysis of the samples was performed by scanning electron microscopy (SEM) and x-ray diffraction (XRD). Sheet resistance of the VCS coatings was measured using a four-point probe method. The influences of TiN additions on the electrical resistivity of SiC-TiN composite coatings and the conductive mechanisms were investigated. The electrical resistivity of SiC-TiN coatings decreases with increasing TiN contents, reaching a minimum of 1.82 Ω m with 50 mol% TiN.

Keywords composite coatings, electrical resistivity, SiC, TiN, vacuum cold spray

1. Introduction

The SiC functional coatings are widely used in microdevices producing high temperature, high voltage, high frequency, and high power due to their excellent properties such as wide band gap, high thermal conductivity and thermal stability, high electrical breakdown field, low thermal expansion rate, and good chemical stability. Moreover, SiC is very compatible with silicon integrated circuit technology (Ref 1-3). However, undoped SiC coatings are not electrically good conductors, which limits the applications of SiC coatings. TiN (Ref 4) is an advanced multi-function ceramic material, and its most prominent advantage is good conductivity (room temperature resistance is about 3.34×10^{-7} Ω cm). Li et al. (Ref 5) reported that the electrical resistivity of TiN-Al_2O_3 nanocomposites prepared by hot-pressing decreased with increasing amounts of TiN and reached a minimum of 6.5×10^{-5} Ω m with 25 vol.% TiN. At present, SiC film doping technologies (CVD, PVD, Ion implantation, etc.) are complex, high temperature, costly, and time-consuming processes (Ref 6-9).

Vacuum cold spray (VCS) is a kind of thick ceramic coating technology based on impact adhesion of ultralfine particles at room temperature. The most outstanding advantages of VCS are its low deposition temperature (room temperature), high deposition rate (ranging from several μm/min to several tens of μm/min for a deposition area of 10 mm × 10 mm), and low cost (Ref 10). VCS is also called Aerosol Deposition (AD) method (Ref 10), which is used to deposit Al_2O_3-based polyimide composite thick films (Ref 11), piezoelectric ceramic-polymer composite thick films (Ref 12), etc. Cuong et al. (Ref 13) reported that the sheet resistivity of TiN film deposited on SiO_2/Si substrates using the reactive magnetron sputtering method is increased from 150 up to 420 Ω when the film thickness decreases from 300 to 50 nm. These values are higher than the sheet resistance (minimum 127 Ω) of the VCS TiN coatings in our lab with the thickness of several tens of microns (Ref 14). In addition, Zhao et al. (Ref 15) also reported the sheet resistances of TiN films prepared by atmospheric pressure chemical vapor deposition, ranging from 34.5 Ω to about 650 Ω. Therefore, VCS can be used to prepare this kind of conductive coating or thick film.

In this study, VCS process was used to deposit nanostructure composite SiC-TiN coatings on Al_2O_3 substrates; the electrical resistivity of SiC-TiN composite layers and the conductive mechanisms were investigated.

2. Experimental Materials and Procedures

2.1 Materials

Nano-sized SiC powders of 40 nm in mean diameter and TiN powders of 20 nm in mean diameter were used as

This article is an invited paper selected from presentations at the 4th Asian Thermal Spray Conference (ATSC 2009) and has been expanded from the original presentation. ATSC 2009 was held at Nanyang Hotel, Xi'an Jiaotong University, Xi'an, China, October 22-24, 2009, and was chaired by Chang-Jiu Li.

Y. Liu, Y.-Y. Wang, G.-J. Yang, and **J.-J. Feng**, State Key Laboratory for Mechanical Behavior of Materials, Xi'an Jiaotong University, Shaanxi 710049, China; and **K. Kusumoto**, Department of Mechanical Systems Engineering, Engineering Faculty of Gunma University, Gunma 376-0052, Japan. Contact e-mail: wangyy@mail.xjtu.edu.cn.

starting materials. SiC-TiN powders with three different TiN contents (molar ratios 10%, 30%, and 50%) were prepared by wet milling in alcohol solution for 10 h and drying at 70 °C for 18 h. Figure 1 shows the morphology of SiC-TiN powders.

An α-Al_2O_3 plate was used as substrate. The sample size is $50 \times 20 \times 1$ mm^3. Prior to spraying, all Al_2O_3 plates were ultrasonically cleaned in acetone solution.

2.2 SiC-TiN Coating Preparation

The SiC-TiN composite coatings were deposited using a VCS apparatus developed in Xi'an Jiaotong University of China. Figure 2 shows the schematic diagram (Ref 16). The VCS system includes a deposition chamber, an aerosol room, a set of vacuum pump, a powder-feeding unit, a particle-accelerating nozzle, a two-dimensional worktable for substrate moving, and a computer control unit. Table 1 gives the spray parameters.

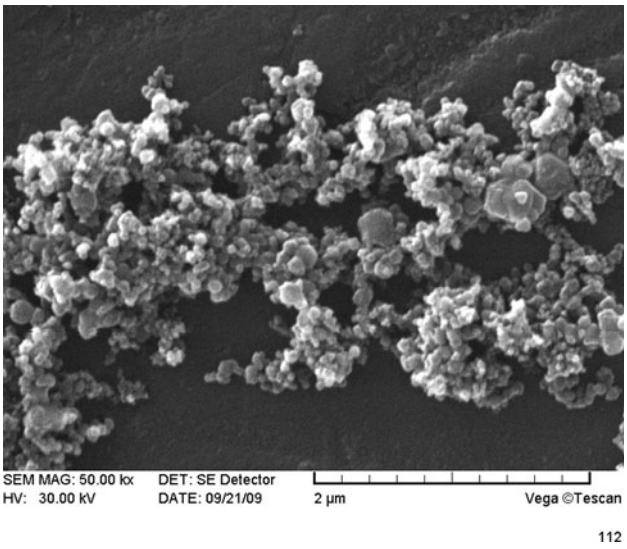

Fig. 1 Morphologies of SiC-TiN powers (50 mol% TiN)

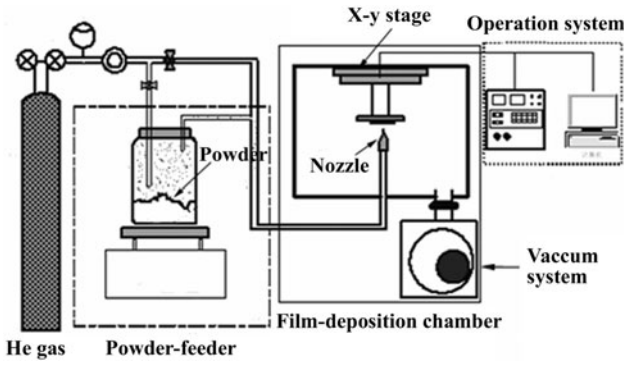

Fig. 2 Schematic diagram of the VCS apparatus (Ref 16)

2.3 Coating Characterization

The cross-sectional morphology of coatings were characterized by scanning electron microscopy (SEM) (TESCAN-VEGA\\XMU, Czech). The phase structure of SiC-TiN powders and coatings were examined by x-ray diffraction (XRD) (Rigaku D/max2400, Japan) with Cu Kα radiation (wavelength is 1.5406 Å) at 40 kV and 100 mA. A scanning rate of 2°/min was used for diffraction angle 2θ.

Table 1 VCS spray parameters

Pressure of deposition chamber, Pa	100
Pressure of aerosol chamber, Pa	2×10^4
He gas flow, L/min	3
Size of nozzle orifice, mm × mm	2.5 × 0.25
Scanning speed, mm/s	1, 3, 5
Spray distance, mm	3, 6, 9

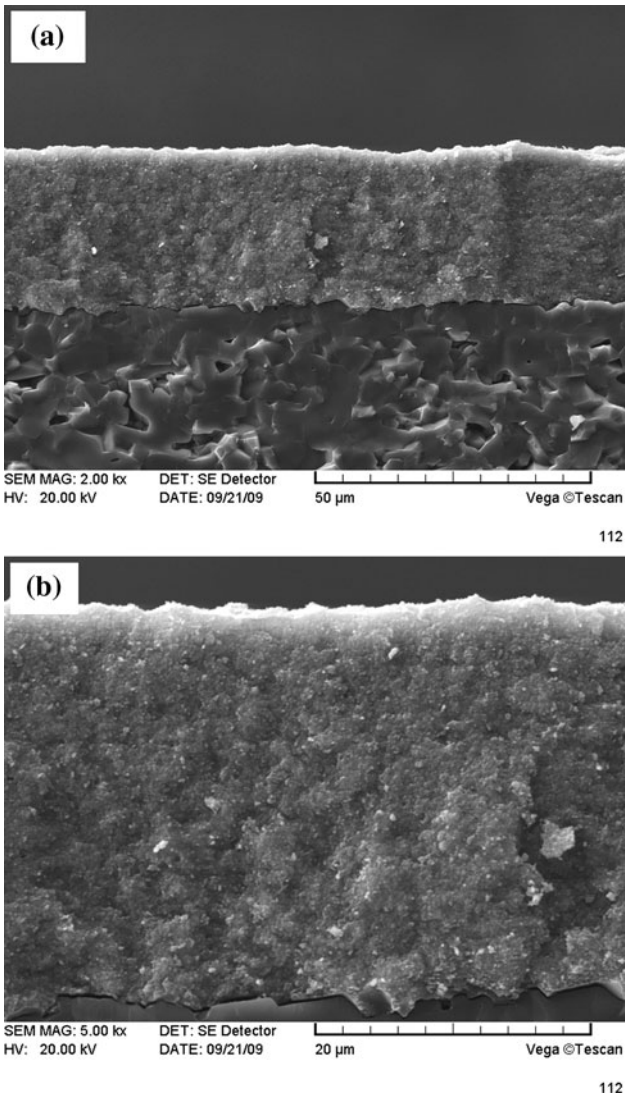

Fig. 3 Fractured morphologies of VCS SiC-50%TiN composite coating ((a) low resolution; (b) high resolution)

The electrical resistivity of SiC-TiN coatings was measured by a double electricity four probes test system (RTS-9, China). The spacing of two adjacent probes is 1 ± 0.01 mm. Influence of coating thickness on sheet resistance is based on the following equation:

$$R = \rho/H \quad \text{(Eq 1)}$$

where R is the sheet resistance, ρ is the electrical resistivity, and H is the coating thickness. The coating thickness is examined by measuring the cross-section of the coating's SEM images.

3. Results

3.1 Microstructure of SiC-TiN Coatings

Figure 3 shows the typical fracture morphologies of the SiC-50%TiN coatings deposited on Al_2O_3 substrates by VCS. The phenomenon of coating spallation and peeling from substrate does not occur during the course of fracturing. It indicates that the composition coating adheres well to the substrate.

Figure 4 shows the XRD patterns of the VCS SiC-50%TiN composite powder and coating. The crystal structure of deposited coatings did not change. However, component of composition coating suffers a little change due to the change in the ratio of peak intensity.

Figure 5 is SEM energy spectrum analysis for cross section of the SiC-50%TiN coatings. SiC was well mixed with TiN. However, the black regions contain more SiC than white regions because Ti is heavier than Si, and the electron scattering for each element depends on their mass. It is indicated that the agglomeration phenomena of SiC particles occurred in several local zones during deposition.

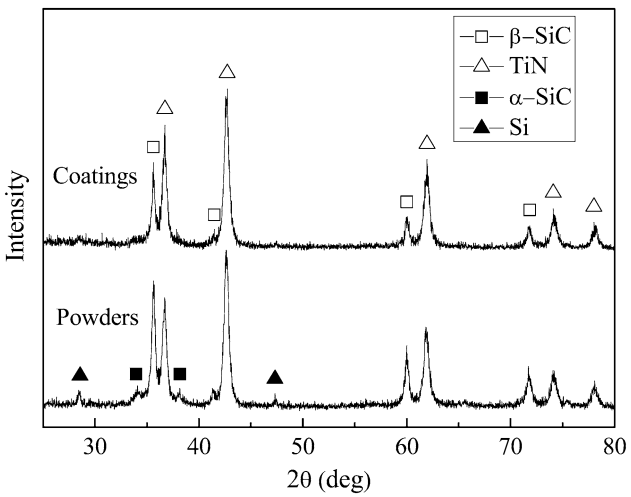

Fig. 4 XRD patterns of SiC-50%TiN nanocomposite powder and coating

3.2 Electrical Properties

Figure 6 shows the influence of spray distance on the electrical resistivity of SiC-50%TiN composition coatings. It is revealed that the minimum is obtained at a spray distance of 6 mm. As the spray distance is increased further, the electrical resistivity of the coatings also increases.

The electrical resistivity of SiC-50%TiN coatings is remarkably decreased with increasing scanning speed (as shown in Fig. 7). The minimum electrical resistivity of

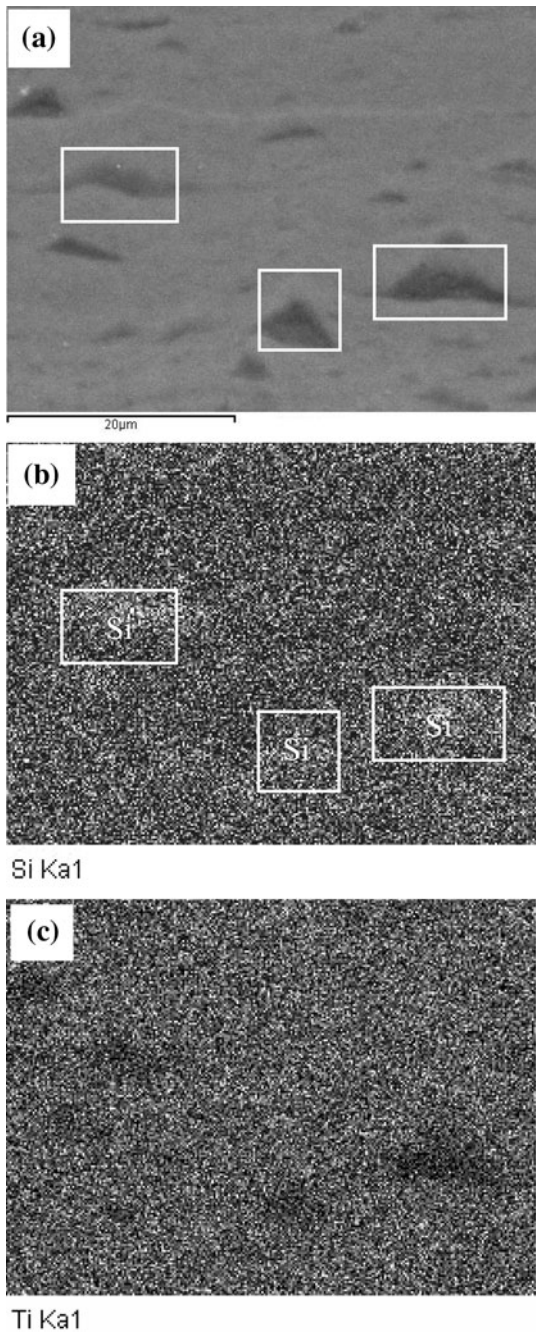

Fig. 5 SEM energy spectrum image of SiC-50%TiN composite coating ((a) Original; (b) Si; (c) Ti)

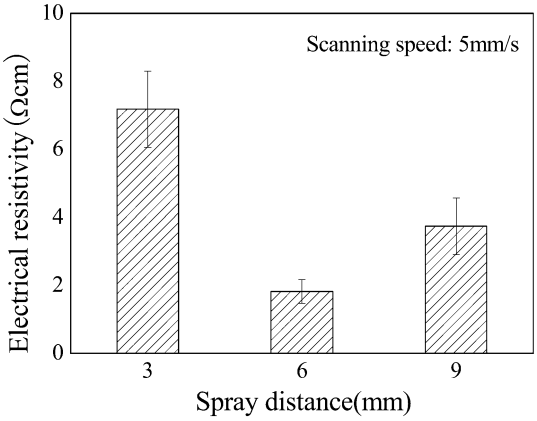

Fig. 6 Influence of spray distance on the electrical resistivity of SiC-50%TiN coating

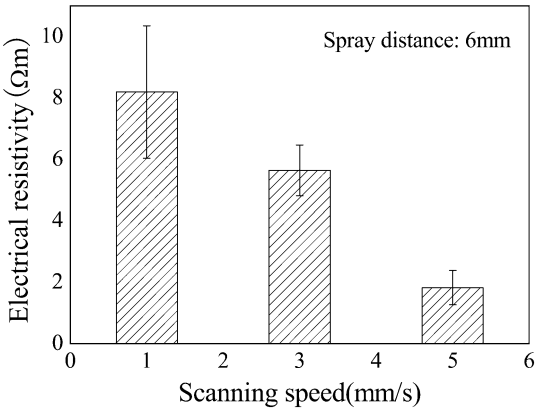

Fig. 7 Influence of scanning speed on the electrical resistivity of SiC-50%TiN coating

1.82 Ω m is achieved at the spray distance of 6 mm and the scanning speed of 5 mm/s.

Figure 8 shows that the electrical resistivity of SiC-TiN coatings is significantly decreased with the increasing TiN contents in the composite coatings. The electrical resistivity of undoped-SiC is of the order of 10^{14} Ω m (Ref 17). The electrical resistivity rapidly decreases to 45.5 Ω m when 10% TiN was added in SiC-TiN composition coatings. A minimum of 1.82 Ω m is obtained with 50 mol% TiN in the SiC-TiN coatings.

The relationship between the sheet resistance and coating thickness of SiC-50%TiN composition coatings is shown in Fig. 9. It is found that the sheet resistance of SiC-TiN coating decreases with increasing the coating thickness. According to the curve in Fig. 9 and the Eq 1, the electrical resistivity with different coating thickness can be estimated.

4. Discussions

Figure 4 reveals that the components of VCS SiC-TiN composite coatings slightly change compared with original

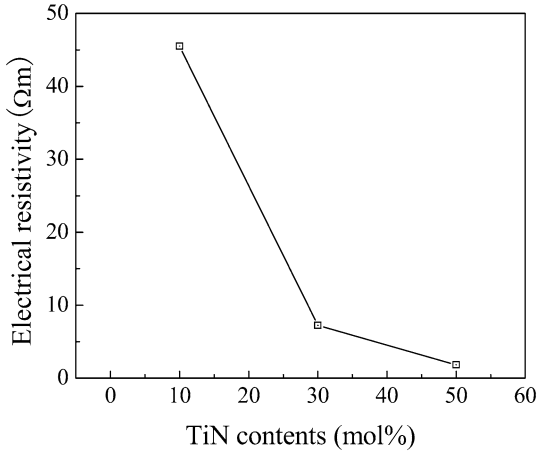

Fig. 8 Effect of TiN contents in the SiC-TiN coating on the electrical resistivity

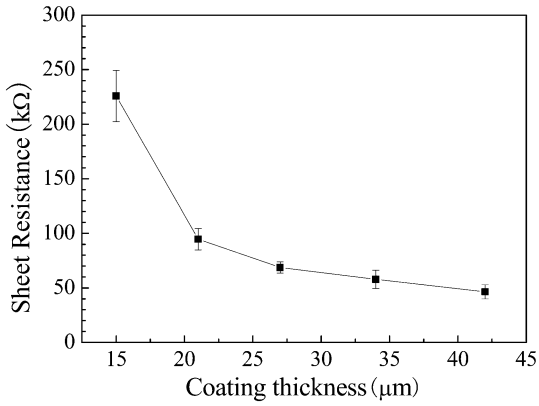

Fig. 9 Effect of the coating thickness on the sheet resistance of SiC-50%TiN coatings

powders because the deposition efficiency is related to the properties of powder such as material type, size, mass, shape, and surface state.

In this study, the optimal parameters are spray distance 6 mm and scanning speed 5 mm/s. Although the effects of spray distance on the velocity of particles are not directly illuminated by experiment at the present, it may be deduced that the particle velocity will increase with increasing spray distance ranging from 3 to 6 mm and then decrease with further increase in the spray distance. The deposited coating presents denser structure with increasing velocity of spray particles due to their higher kinetic energy (Ref 18). Therefore, the porosities and gaps in the coatings reduce significantly. As a result, the minimum electrical resistivity of SiC-TiN coatings is achieved at the spray distance of 6 mm. The lower scanning speed implies more spray particles impacting simultaneously the same zone on the substrate at every spray pass. It is indicated that a thicker layer is deposited after one pass, which leads to the tamping effect of the subsequent particles being significantly impaired. In consequence, the cohesion between the thicker layers and particles in the layers is

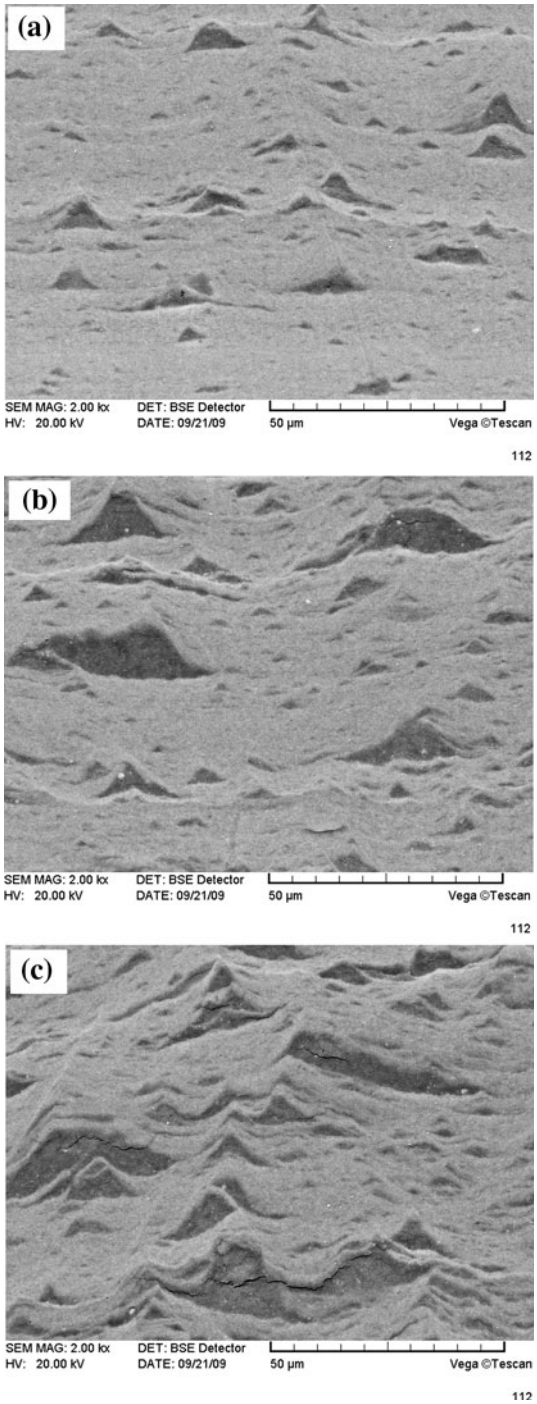

Fig. 10 Cross-sectional images for BSE of SiC-TiN composite coating ((a) SiC-10%TiN; (b) SiC-30%TiN; (c) SiC-50%TiN)

seriously weakened. Therefore, high scanning speed has contributed to the uniformity and compaction of coating which is important for electron-transporting.

Figure 10 shows the cross-sectional BSE images of VCS SiC-TiN composite coatings with different TiN contents. It is found that the black SiC-enrichment regions present triangles. Figure 11 shows schematically the spray particle deposition process. Comparing to the morphology of the

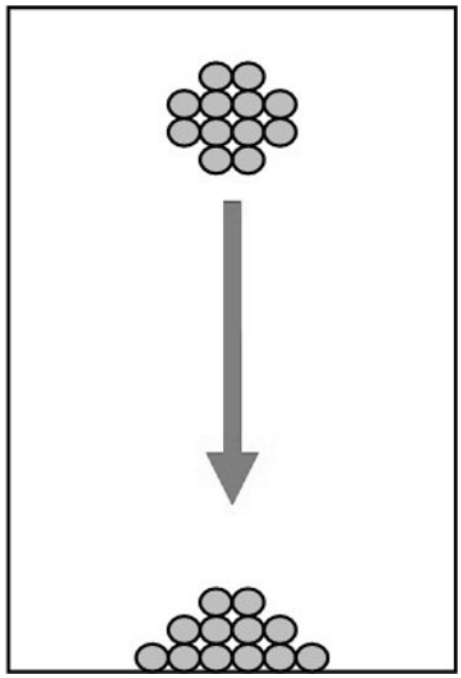

Fig. 11 Schematic diagram of particle deposition process in VCS

SiC-TiN composite powders (shown in Fig. 1), the nano-sized particles are first prone to agglomerate singly into the larger particles after mechanical mixing owing to their high ratio surface area and high surface energy. It is based on the assumption that the larger agglomerated ceramic particles are accelerated by gas flow in the nozzle up to a relatively low velocity during spraying causing impact on the substrate. These larger agglomerated particles slightly deform due to the lower kinetic energy. Actual deposition mechanism of single particle has not been clarified.

SiC-TiN conductive coatings were successfully fabricated by VCS, but what is the conductive mechanism? Both the SiC and TiN powders are ultralfine. It can be observed from Fig. 5 that the TiN-conductive phase homodisperses in the whole area, and the insulating phase exhibits partial agglomeration. Figure 12 schematically shows the distribution of the two-phase particles. The conductive particles contact and connect each other to form many channels for electron-transporting. Assuming that TiN powders present are in the state of agglomeration, they cannot form net-like structure which provides the channels for electron-transporting. Therefore, the conductive phase homodisperses in the whole region and form a net-like structure, which contributes to the electron-transporting.

5. Conclusion

The SiC-TiN nanocomposition coatings with different TiN contents were successfully fabricated on Al_2O_3 substrates by vacuum cold spray at room temperature. The

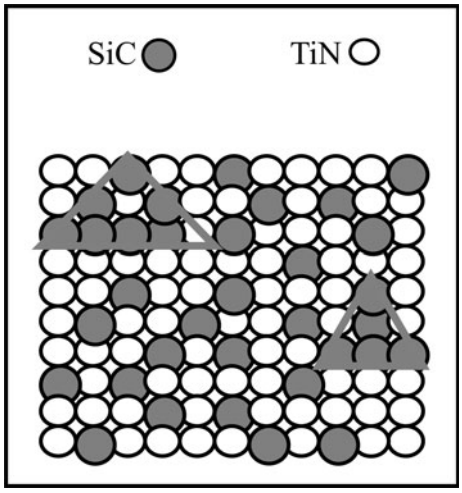

Fig. 12 Schematic diagram of the particles distribution

original crystal structure of SiC-TiN composite powder can be retained after deposition. The electrical resistivity rapidly decreases from the order of 10^{14} to 45.5 Ω m when SiC-TiN composition coating was added with 10 mol% TiN. The electrical resistivity of coatings is significantly decreased with increasing TiN contents in the composite coatings. A minimum of 1.82 Ω m is achieved with 50 mol% TiN in the SiC-TiN coatings at the spray distance of 6 mm and the scanning speed of 5 mm/s. The conductive phase homodisperses in the whole region and forms a net-like structure, which contributes to the electron-transporting.

Acknowledgment

The present research project was supported by National Natural Science Foundation of China (Granted No. 50705075).

References

1. J.-C. Zhou, X.-Q. Zheng, and F. Liu, The Latest Research Progress of SiC Films and Devices Membrane, *Mater. Rev.*, 2007, **21**(3), p 112-118 (in Chinese)
2. G.-S. Chung and J.-H. Ahn, Characterization of Polycrystalline 3C-Sic Thin Film Diodes for Extreme Environment Applications, *Microelectron. Eng.*, 2008, **85**, p 1772-1775
3. X.-Y. Cui, Development of SiC and Its Process, *J. Rev. Prospect*, 2007, **25**(4), p 58-62 (in Chinese)
4. R.-H. Yu and M.-X. Jiang, The Properties and Applications of TiN and the Fabrication Methods of TiN Powders, *Refract. Mater.*, 2005, **39**(5), p 386-389 (in Chinese)
5. J.-G. Li, L. Gao, and J.-Q. Guo, Mechanical Properties and Electrical Conductivity of Tin-Al_2O_3, *J. Inorg. Mater.*, 2002, **17**(6), p 1215-1219 (in Chinese)
6. Y. Hoshide, A. Tabata, A. Kitagawa, and A. Kondo, Preparation of N-Type Nanocrystalline 3C-Sic Films by Hot-Wire CVD Using N_2 as Doping Gas, *Thin Solid Films*, 2009, **517**, p 3524-3527
7. C. Serrea, D. Pankninb, A. Pérez-Rodrígueza, A. Romano-Rodrígueza, J.R. Morantea, R. Köglerb, W. Skorupab, J. Estevec, and M.C. Aceroc, Ion Beam Synthesis of N-Type Doped Sic Layers, *Appl. Surf. Sci.*, 2001, **184**, p 367-371
8. J.-C. Zhou and X.-Q. Zheng, Structure and Electronic Properties of Sic Thin-Films Deposited by RF Magnetron Sputtering, *Trans. Nonferrous Met. Soc. China*, 2007, **17**, p 373-377
9. Z. Tian, I.A. Salama, N.R. Quick, and A. Kar, Effects of Different Laser Sources and Doping Methods Used to Dope Silicon Carbide, *J. Acta Mater. Inc*, 2005, **53**(9), p 2835-2844
10. J. Akedo, Aerosol Deposition of Ceramic Thick Films at Room Temperature—Densification Mechanism of Ceramic Layer, *J. Am. Ceram. Soc.*, 2006, **89**(6), p 1834-1839
11. H.J. Kim, Y.J. Yoon, J.H. Kim, and S.M. Nam, Application of Al_2O_3-Based Polyimide Composite Thick Films to Integrated Substrates Using Aerosol Deposition Method, *Mater. Sci. Eng. B*, 2009, **161**, p 104-108
12. J.-J. Choi, B.-D. Hahn, J. Ryu, W.-H. Yoon, B.-K. Lee, and D.-S. Park, Preparation and Characterization of Piezoelectric Ceramic-Polymer Composite Thick Films by Aerosol Deposition for Sensor Application, *Sens. Actuators A*, 2009, **153**, p 89-95
13. N.D. Cuong, D.-J. Kim, B.-D. Kang, C.S. Kim, and S.-G. Yoon, Characterizations of High Resistivity TiN_xO_y Thin Films for Applications in Thin Film Resistors, *Microelectron. Reliab.*, 2007, **47**, p 752-754
14. Y.-Y. Wang, Y. Liu, C.J. Li, G.J. Yang, J.J. Feng, and K. Kusumoto, Effect of Microstructure on the Electrical Properties of Nano-Structured TiN Coatings Deposited by Vacuum Cold Spray, *Proceedings of the 4th Asian Thermal Spray Conference*, China, October 22-24, 2009, p 392-398
15. G. Zhao, T. Zhang, T. Zhang, J. Wang, and G. Han, Electrical and Optical Properties of Titanium Nitride Coatings Prepared by Atmospheric Pressure Chemical Vapor Deposition, *J. Non-Cryst. Solids*, 2008, **354**, p 1272-1275
16. S.-Q. Fan, G.-J. Yang, C.-J. Li, G.-J. Liu, C.-X. Li, and L.-Z. Zhang, Characterization of Microstructure of Nano-TiO_2 Coating Deposited by Vacuum Cold Spraying, *J. Therm. Spray Techn.*, 2006, **15**(4), p 513-517
17. G.-L. Sun, G.-H. Xia, and P.-J. Li, The Composition of SiC Electrical Heating Ceramic and Electric Conductivity, *J. Ceram. Stud.*, 1999, **14**(4), p 9-14 (in Chinese)
18. K.-X. Liao, Influence of Powder Structure and Accelerating Gas Flow on Electron Transport Property of Nanostructured TiO_2 Films Deposited by Vacuum Cold Spray, Master thesis, Xi'an Jiaotong University, May 2010, p 28-31